LANGMUIR

Article

pubs.acs.org/Langmuir

Tether-Length Dependence of Bias in Equilibrium Free-Energy Estimates for Surface-to-Molecule Unbinding Experiments

Laila Moreno Ostertag,[†,∥] Thomas Utzig,[†,∥] Christine Klinger,[‡] and Markus Valtiner*[,†,§]

[†]Interaction Forces and Functional Materials, Department of Interface Chemistry and Surface Engineering, Max-Planck-Institut für Eisenforschung GmbH, 40237 Düsseldorf, Germany

[‡]Institut für Physikalische Chemie II, TU Bergakademie Freiberg, 09599 Freiberg, Germany

[§]Institute for Applied Physics, Applied Interface Physics, Technical University of Vienna, 1040 Vienna, Austria

ABSTRACT: The capabilities of atomic force microscopes and optical tweezers to probe unfolding or surface-to-molecule bond rupture at a single-molecular level are widely appreciated. These measurements are typically carried out unidirectionally under nonequilibrium conditions. Jarzynski's equality has proven useful to relate the work obtained along these nonequilibrium trajectories to the underlying free energy of the unfolding or unbinding process. Here, we quantify biases that arise from the molecular design of the bond rupture experiment for probing surface-to-molecule bonds. In particular, we probe the well-studied amine/gold bond as a function of the linker's length which is used to anchor the specific amine functionality during a single molecule unbinding experiment. With increasing linker length, we observe a significant increase in the average work spent on polymer stretching and a strongly biased estimated interaction free energy. Our data demonstrate that free energy estimates converge well for linker lengths below 20 nm, where the bias is <10−15%. With longer linkers severe methodical limits of the method are reached, and convergence within a reasonable number of realizations of the bond rupture is not feasible. Our results also provide new insights into stability and work dissipation mechanisms at adhesive interfaces at the single-molecular level, and offer important design and analysis aspects for single-molecular surface-to-molecule experiments.

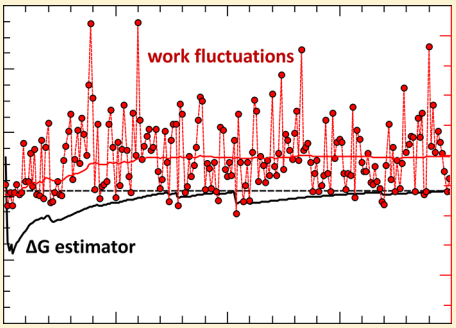

INTRODUCTION

Single-molecule force spectroscopy (SM-AFM) using an atomic force microscope or optical tweezers has been state of the art for about 20 years now providing direct access to molecular unbinding rates and interaction free energies.[1−10] In a typical SM-AFM experiment, polymer molecules of interest that are functionalized with a specific binding group are immobilized on flat surfaces, AFM tips, or microscopic beads in such a way that they can specifically bind to opposing designed surfaces. Figure 1 shows a typical bond rupture experiment and process as recorded using a force probe device. Application of a mechanical force F induces molecular stretching of the polymeric tether and subsequent bond dissociation. Experimental data typically extracted from these experiments are bond rupture forces F_B and resulting characteristics of unbinding kinetics[4] on a single-molecular level, and the work W_n transferred into the molecular system during the rupture event.

One of the major challenges in interpreting these experiments is that the applied mechanical force drives the system into an *out of thermodynamic equilibrium* bond rupture event. In order to rationalize the molecular process and measured quantities, it is instructive to consider how energy is transferred and dissipated during the molecular process shown in Figure 1. First, the loading of the molecular linker (step 1 and 2 in Figure 1) by an external spring (e.g., the AFM cantilever) is an equilibrium process. The molecular relaxation times of the molecular linker are much faster compared to the motion of the AFM cantilever. Hence, the energy transferred during bond loading is essentially equal to the work stored in the molecular spring. Depending on the loading rate and the characteristics of the molecular bond, unbinding occurs with a rather broad unbinding force, F_B, and work (W_n) distribution. Upon bond rupture, the work stored in the molecular tether dissipates during tether relaxation back into the thermodynamic configuration. In addition, the bond breaks against the binding energy, and after equilibration the bond energy constitutes the resulting interaction free energy change between the bound and the unbound state (free energy difference between configurations in step 1 and 4 in Figure 1). In total, the work that is transferred into the molecular system under equilibrium conditions during tether loading and until bond rupture occurs, is hence equal to the sum of the dissipated work due to tether relaxation and the bond breaking energy realized during

Special Issue: Early Career Authors in Fundamental Colloid and Interface Science

Received: August 11, 2017
Revised: October 30, 2017
Published: October 31, 2017

DOI: 10.1021/acs.langmuir.7b02844
Langmuir 2018, 34, 766−772

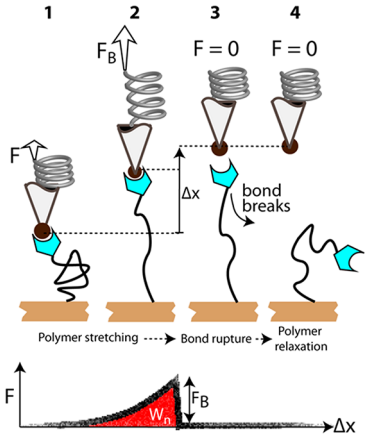

Figure 1. Schematic of consecutive processes during a molecular unbinding experiment of a surface-to-molecule bond. A specific bond between a functional group, which is grafted to a single polymer linker (e.g., polyethylene glycol), and a surface (here an AFM tip) can be broken upon application of a mechanical force using force probe experiments. Upon retraction of the force probe away from the surface, the polymeric linker extends out of its equilibrium configuration resulting in force measurable with a spring-based device. The work transferred into the molecular system is characterized by the integral $W_n = \int F\Delta x$. This polymer extension process is an equilibrium process. Upon bond rupture, the work transferred into the system dissipates during instant polymer relaxation and bond rupture, transferring the system into an unbound thermodynamic equilibrium state (cf. text for details).

practically (on the time scale of a force probe experiment) instantaneous bond rupture.

Both measured rupture forces and work depend on experimental loading rates,[4] and the average work extracted from these experiments $\langle W \rangle$ is an upper bound for the underlying free energy ΔG_0 as evident from Clausius' inequality: $\langle W \rangle > \Delta G_0$. It has been pointed out that application of Jarzynski's equality[11−13] (JE, eq 1) is extraordinary useful to determine this central thermodynamic quantity:

$$e^{-\Delta G_0/k_BT} = \left\langle e^{-\int F dz/k_BT} \right\rangle_n \quad (1)$$

Here, k_B represents Boltzmann's constant, T the temperature, and z indicates the pulling coordinate. JE relates the work spent in any nonequilibrium process $W_n = \int F\,dx$ to the underlying free-energy by exponentially averaging over many work trajectories n. For $n \to \infty$, this average converges to the exponent of ΔG_0. This method has been successfully applied to describe the energetics of molecular stretching and bond dissociation as measured with molecular tethers.[14−17] Hence, exponential averaging of the work during a process from one equilibrium state to another, here from step 1 to 4 in Figure 1, provides a direct route to estimating interaction free energies of bond that can be broken by force probe experiments. Also, the closer to thermodynamic equilibrium a process is driven, the easier the convergence of the Jarzynski sum is.

In experimental reality, however, n always remains finite, and experimental procedures are often far from thermodynamic equilibrium, leading to a potential bias of calculated free energies using JE. Jarzynski and others attempted to quantify the errors caused by a finite number of trajectories. Particularly, they specify how large n has to be in order to calculate ΔG_0 correctly and emphasize the importance of "bidirectionality" (involves quantification of forward and reverse trajectories of the process of interest) to significantly improve the results.[18−23] Even though experiments performed on reversible RNA unfolding/refolding using optical tweezers have been able to match the criterion of bidirectionality[24] it cannot be applied to every process.

In particular, for the interesting question of adhesion of molecules at solid/liquid interfaces, only unbinding trajectories (forward) are measurable while binding trajectories (reverse) have not been observed to our knowledge. In these cases, one faces the difficulty that low work values corresponding to rare unbinding events can potentially dominate the estimate of ΔG_0.[25] In addition, the measured overall dissipated work W_n during a process from 1 to 4 (see Figure 1) typically includes both the work dissipated during molecular tether folding and the work spent on bond rupture.[26] As a result, the longer the linker is, the further out of equilibrium the system is during bond rupture. Hence, one expects significantly less efficient convergence of the measured interaction free energy for longer linkers.

Here, we experimentally quantify systematic errors that arise from the molecular design of bond rupture experiments for probing surface-to-molecule bonds. In particular, we probe the well-studied amine/gold bond as a function of the linker's

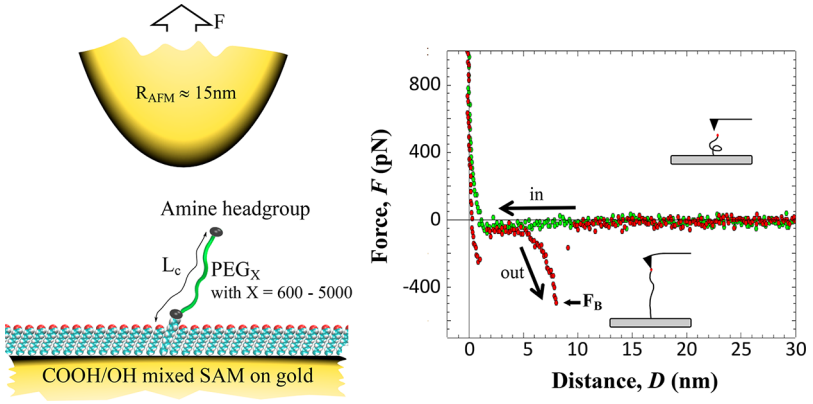

Figure 2. Experimental model system used to probe the amine/gold interaction at various linker contour lengths (L_C). Bifunctional PEG_X amines (X = 600, 2000, 3400, and 5000) are immobilized on a COOH/OH mixed SAM (COOH/OH = 1/500 for PEG_{600} and PEG_{2000} or COOH/OH = 1/1000 for PEG_{3400} and PEG_{5000}). Right: Force trajectory showing a single molecular unbinding event represented by the pronounced adhesive minimum in the retraction curve (red dots).

DOI: 10.1021/acs.langmuir.7b02844
Langmuir 2018, 34, 766−772

length, which is used to anchor the specific amine functionality during a single molecule unbinding experiment as shown in Figure 2. Our results reveal a strong influence of the linker length and demonstrate how experimental design can minimize the effect of the linker used.

EXPERIMENTAL SECTION

Chemicals and Materials. All chemicals used are of highest grade and are used without further purification (Supplier: Sigma-Aldrich). Milli-Q water (Merck Millipore purification system) is used to prepare 5 mM NaCl solution for AFM experiments with a resistance of 18.2 MΩ cm and a TOC content of 2 pbb. 11-Mercapto-1-undecanol (OH-terminated thiol) and 16-Mercaptohexadecanoic acid (COOH-terminated thiol) of highest available purity are obtained from Sigma-Aldrich.

Surface Preparation. Molecularly smooth gold surfaces are prepared by template stripping from Mica as previously described.[27] Surface modification is carried out following an established protocol.[28−30] First the freshly stripped surfaces are immersed into an ethanolic solution of a 1/500 or 1/1000 mixture of COOH- and OH-terminated thiol, respectively. After more than 12 h of exposure surfaces are removed from the self-assembled monolayer (SAM) solution, rinsed with ethanol, hexane, and ethanol and dried in a gentle N_2 stream. Further modification is carried out by covalently binding homobifunctional polyethylene glycol (PEG)-amines of different lengths (Supplier: Nanocs, New York, USA) to the SAM's free COOH groups. For this purpose, the surfaces are immersed into phosphate buffered saline (PBS) buffer solution containing the corresponding PEG-amine, *N*-(3-(dimethylamino)propyl)-*N*′-ethyl-carbodiimide hydrochloride (EDC), and *N*-hydroxysuccinimide (NHS) for at least 2 h. Afterward, the surfaces are washed intensively with PBS solution, water, and ethanol, dried in an N_2 stream, and immediately mounted into the AFM cell. XPS and AFM characterization of the mixed SAM and diamines immobilized on the mixed SAM is available elsewhere.[6] For experiments involving the shorter PEG-amines (PEG_{600} and PEG_{2000}), the COOH/OH ratio in the mixed SAM is adjusted to 1/500, while, for experiments involving the longer PEG-amines (PEG_{3400} and PEG_{5000}), a ratio of 1/1000 is used to avoid abundance of multimolecular rupture events.

AFM Tip Preparation. All experiments are carried out using rectangular gold-coated cantilevers (CONTGB-G, BudgetSensors). Each tip is cleaned with 95% concentrated sulfuric acid, two batches of water, and one batch of ethanol for 60 s each and dried gently in an N_2 stream. After drying, the tips are mounted immediately into the AFM setup to perform experiments.

AFM Force Spectroscopy and Data Analysis. All experiments are carried out in a 5 mM NaCl electrolyte with an adjusted pH of ≈ 4. We use a Nanowizard AFM (JPK Instruments, Germany). The AFM cantilever's sensitivity is extracted from the linear regime of at least seven approach curves, and its spring constant is determined using the thermal noise method.[31] Typical spring constants vary between 250 and 500 pN/nm with a sensitivity of 65 to 100 nm/V. Sensitivity and spring constant are used to convert the raw cantilever deflection versus tip−sample separation data into force−distance profiles. The closest approach is set to $D = 0$. Force runs are recorded at constant speed in a square grid pattern with 10 × 10 points separated by 10 nm. At each point 10 force curves are recorded. In total at least 8000 curves are obtained for each experiment from different sample locations. The maximum force applied during approach is set to 1 nN to ensure tip/surface contact and maximize the probability of single-molecule pick-up. The experimental loading rate is adjusted for each experiment to 178 nN/s, unless otherwise mentioned. All data are recorded and processed using JPK data processing software. All measured force profiles showing single-molecular pulling (5−20% depending on the used PEG-amine and sample location) are collected and aligned to the WLC model (see Figure 3 and 4). Work values are integrated by using a numerical integration based on the trapezoidal method.

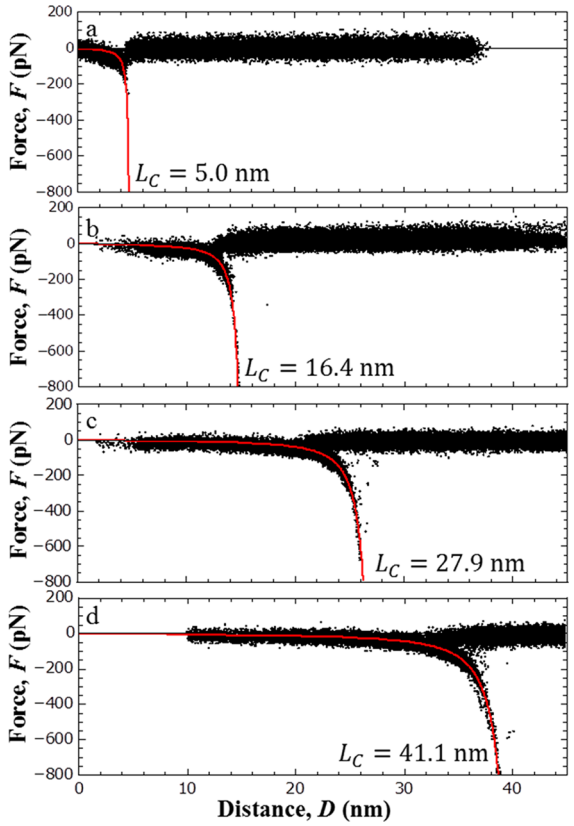

Figure 3. Force−distance trajectories exhibiting single-molecular unbinding events aligned to the Worm-like chain model (solid red line, persistence length: L_P = 0.37 nm). (a) PEG_{600} with L_C = 5.0 nm. (b) PEG_{2000} with L_C = 16.4 nm. (c) PEG_{3400} with L_C = 27.9 nm. (d) PEG_{5000} with L_C = 41.4 nm.

RESULTS AND DISCUSSIONS

In this work we experimentally characterize work distributions and estimate the free energy associated with rupture of molecular interactions at a solid/liquid interface using monodisperse PEG tethers of variable lengths. The utilized experimental model system is shown in Figure 2. We immobilize bifunctional amine-terminated PEG on mixed SAMs consisting of COOH- and OH-terminated thiols in a 1/500 or 1/1000 ratio. The immobilized PEG is amine-functionalized at both ends. One of the free amines is used to covalently bind PEG to the mixed SAM via EDC- and NHS-assisted coupling reactions[28,29] (see experimental section for details), while the other amino-group remains free. Such a modified surface faces a gold-coated AFM tip that interacts with the free amines via the well-studied amine/gold bond.[32−36] This interaction has been studied by us and others, and its binding energy has been estimated by other methods to be 36−37 k_BT.[32,34]

The used PEG-amines are available in a wide range of molar mass and thus PEG chain length. Monodisperse PEG derivatives used in this study are of molar mass 600, 2000, 3400, and 5000 g/mol corresponding to contour lengths (L_C) of 5, 16.4, 27.9, and 41.4 nm (see Figure 2). As such, this model system allows us to measure amine/gold unbinding using SM-AFM as a function of the linker's chain length. Here, we specifically focus on characterizing force histograms, and resulting biases at a given set of 200 force trajectories as a function of the tether length.

DOI: 10.1021/acs.langmuir.7b02844
Langmuir 2018, 34, 766−772

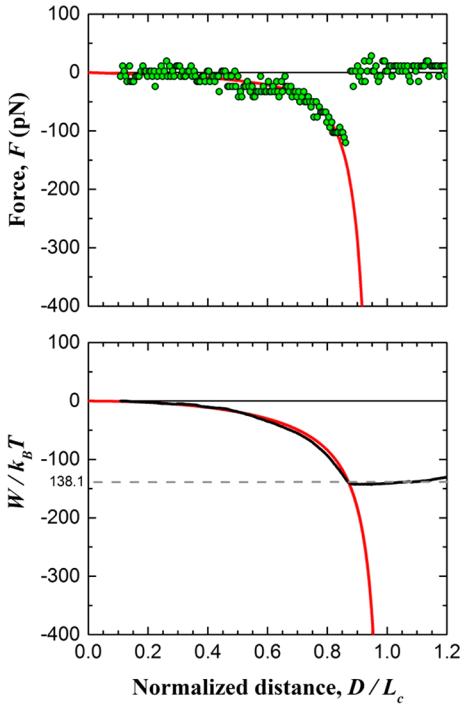

Figure 4. Typical integration of a single molecular rupture trajectory for a PEG_{3400} system. Note that the distance is normalized by the contour length. The top panel shows a force curve aligned with the WLC fit. The bottom shows the integration of both the data and the WLC fit. Clearly, the work transferred into the molecular system is essentially the energy stored in the stretched tether during bond loading.

The force plot in Figure 2 depicts a measured full force trajectory exhibiting a single-molecular unbinding event. The green curve represents the force signal, while the AFM tip approaches the modified surface. Here, no pronounced interaction is visible, and the force profile is dominated by integral interactions between the tip and the extended surface (Van-der-Waals and electric-double-layer interactions). Upon retraction of the AFM tip (red curve in Figure 2), a primary adhesive minimum below 1 nm distance has to be overcome to separate tip and surface, which is again attributed to integral background interactions. If an amine/gold bond between the PEG-amine and the AFM tip is formed, a second, pronounced minimum is visible, which is attributed to stretching the PEG chain, which stores the energy for breaking the amine/gold bond until bond rupture at the breaking force F_B. Depending on the PEG chain length, these events are visible in 5−20% of the recorded force trajectories.

All force curves exhibiting these single-molecular rupture features are further analyzed and aligned to the Worm-like chain model (WLC) as shown in Figure 3.[37] Panels a, b, c, and d correspond to different chain lengths of 5, 16.4, 27.9, and 41.4 nm, respectively. The WLC model serves as unambiguous identifier of the mechanical properties of PEG, which undergoes a forced equilibrium transition between a random and a stretched configuration. These properties are well known[38] and as such the WLC model is suitable to identify single-molecular stretching followed by amine/gold rupture. Figure 3 further shows that bond rupture shifts to longer distances for longer linkers as expected.

All force trajectories shown in Figure 3 are analyzed using JE (eq 1). Therefore, the work W_n transferred during each pulling and bond rupture event is extracted from the force−distance behavior by integration of the specific part of the force curve. The integration runs from the instance when the AFM tip picks up a molecule with the cantilever being in zero position until post bond rupture with the cantilever in zero position again. Figure 4 shows a typical integration of a force curve and compares it to the energy stored in the spring. As can be seen, W_n contains essentially the contribution from stretching the PEG molecule in the experimental environment (5 mM NaCl of pH ≈ 4), which will release and dissipate upon bond rupture of the amine/gold bond.[26] W_n constitutes the total work transferred to the molecular system for the realization of the experimental rupture process. It is hence the direct measure for work that is necessary to transfer the system from the equilibrated state in close contact (step 1 in Figure 1) to the fully equilibrated state after bond rupture occurred as shown in Figure 1.

By averaging the exponential of these work values, one in principle exactly obtains the free energy between two equilibrium states at the end of any (nonequilibrium) process based on JE. Our beginning state for integration consists of a relaxed linker and amine/gold interacting at the tip interface. The end state corresponds to both the linker and amine-PEG similarly relaxed (i.e., under no tension) but with the tip far away from the surface. Thus, the difference between the two states consists of the presence of a specific amine/gold interaction. Please note that more rigorous methods of extracting W_n from force−distance data and unraveling the evolution of ΔG_0 along the pulling coordinate are discussed elsewhere,[39,40] here we integrate the mechanical work.

In any case, Jarzynski relation does not require special treatment or modification in light of the nature of the intervening nonequilibrium process, and this is its great strength. Indeed, free energy differences are insensitive to the nature of events during the pathways that are intermediate between the beginning and ending states. While the average total and average dissipative work $\bar{W}_{dis} = (\langle W \rangle - G_0)$ grows significantly with the extent of nonequilibrium effects such as increasing tether lengths, the distribution of work values will also change so as to preserve the underlying free energy. This makes it more and more complicated and often experimentally not feasible to properly sample a work distribution, resulting in a significant bias of the estimated free energy.[41]

Figure 5a shows the measured work histograms for the four different linker lengths. Even though in all experiments the amine/gold bond is probed, the work distributions vary significantly as a function of the used linker length. With increasing length, the distributions broaden and the maximum shifts to higher work values. As a side note, this result has interesting implications for adhesion science in general. Even if the adhesive bond is similar, the energy dissipation during bond rupture can significantly increase forces and hence dissipative work of adhesion that are necessary for unbinding an adhesive junction. As such, controlling interfacial polymer structures of adhesives will offer a strategy for controlling adhesive forces.

Further, comparing the average work and the JE estimate in Figure 5b for the four different chain lengths reveals a significant increase of both average work and estimated interaction free energies (eq 1) upon evaluation of 200 work trajectories for every linker length. Specifically, the red curve in Figure 5b shows the calculated ΔG_0 using JE as a function of the PEG linker's length. Based on the experimental samples we observe an increasing ΔG_0 from 34 k_BT for the shortest linker

DOI: 10.1021/acs.langmuir.7b02844
Langmuir 2018, 34, 766−772

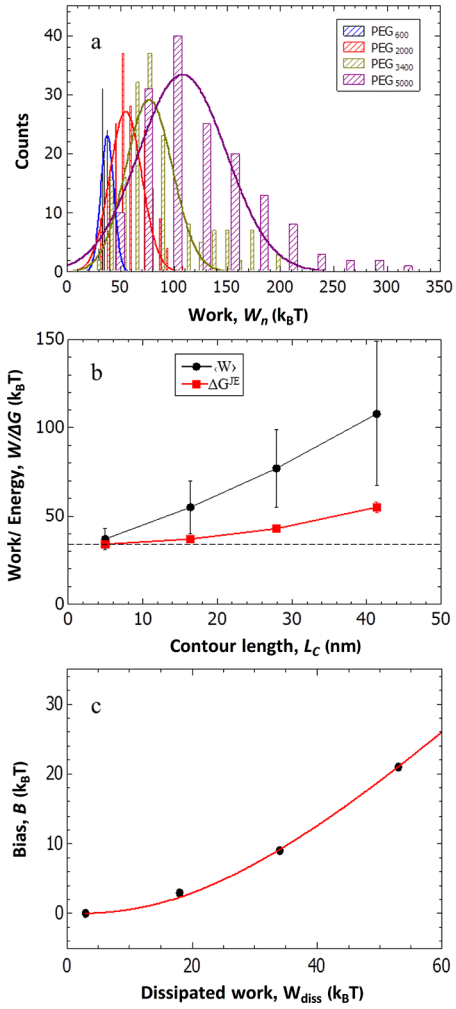

Figure 5. (a) Measured work distributions for various linker lengths. (b) Evolution of the average work (black) and the estimated free energy using Jarzynski's equality (red). (c) Estimated experimental bias as a function of the dissipated energy $W_{Diss} = \langle W \rangle - \Delta G_0^{JE}$. The red line is a guide for the eye.

to 55 k_BT for the longest linker. In a previous study we estimated ΔG_0 for an almost identical system to be 36−37 k_BT,[32] which is also in good agreement with the results obtained by other groups.[34]

Consequently, the work distributions for longer linkers are not well sampled with 200 trajectories, and estimates for ΔG_0 are clearly biased for long linkers. This is possibly due to larger deviations from thermodynamic equilibrium during relaxation of the longer linkers from larger rupture distances. This is not unexpected since longer molecules have more degrees of freedom in a good solvent (which is the case for PEG in water), and as such the transition from a random orientation to a fully stretched chain is entropically less favorable and more work has to be spent, and hence dissipates, for this process on average.

The increasing ΔG_0 clearly shows that the work spent on the linker folding biases the estimated ΔG_0. The quantity of interest from an interface science point of view is the interaction free energy of the underlying bond rupture. We can now estimate the experimental bias by accepting 34 k_BT measured by a different group[34] as a good estimate for the underlying amine/gold binding energy. We can than estimate the dissipated work by subtracting the average work and the best estimate for ΔG_0 (subtracting 34 k_bT from the black curve in Figure 3b). As expected, the bias increases with increasing dissipated work. For the longest linker used the bias is ∼60% of the expected value.

We can now also estimate the bias of the measured work distribution shown in Figure 5a based on the work by Gore et al.[41] In our system, the bias can be estimated as $\frac{\bar{W}_{dis}}{N^{\alpha}}$ with the factor $\alpha = \frac{\ln[2C\bar{W}_{dis}/kT]}{\ln\left[C\left(\exp\left(\frac{2\bar{W}_{dis}}{kT}\right)-1\right)\right]}$ depending on the average dissipated work, and $C = 15$ is a constant.[41] For PEG_{600}, with $G_0 \sim 34$ kT based on our and other work,[35] $\langle W \rangle = 39.8$ kT and hence $\bar{W}_{dis} = 5.8$ kT we can estimate an expected bias of only ∼1 kT. By contrast, the measured $\bar{W}_{dis}$ of 38 kT, 71 kT, and 114 kT, and hence the resulting statistically expected bias increases significantly to 25 kT, 55 kT, and 95 kT for PEG_{2000}, PEG_{3400}, and PEG_{5000}, respectively, for the probed 200 realizations of the process. Experimentally, however, we find lower biases of 3.5 kT, 4 kT, and 21 kT, respectively. This is important, as it suggests that the estimated free energies for the longer PEG chains are significantly lowered by random small work values, which can artificially lower the expectation value. As mentioned above, this again indicates incomplete sampling for the longer PEG chains that are probed further from equilibrium. We can hence conclude that 200 realizations of surface-to-molecule rupture experiments are only enough if the PEG chain length is kept as short as possible. As a caveat, it is important to note that the expression derived by Gore et al. is only valid for near-equilibrium experiments. It is not clear if this is the case for increasing linker lengths. Clearly, the results suggest a departure from close-to-equilibrium conditions. Unfortunately, there is no analytical expression for estimating biases far from equilibrium. As such, the biases estimated above are possibly even underestimated for the increasing linker length.

Based on the experimentally obtained $\bar{W}_{dis}$, it is now interesting to consider how many realizations of the bond rupture are necessary for a proper sampling of the work histograms, and how this compares to our experiments. Gore et al.[41] estimated the bias as a function of the number of trajectories for different average dissipated works. Specifically, a bias of less than 1 kT can be obtained for $\bar{W}_{dis} < 8$ kT within about 100 realizations of the process. This agrees well with the observed behavior of PEG_{600} shown in Figure 6. Within about 50−100 force trajectories we obtain a stable value that is not biased by low numbers. Specifically, and as can be seen in Figure 6 as well, about 20% of the values are in fact lower compared to the JE estimate, indicating proper sampling of the work histograms. For PEG_{3400}, already more than 10^6 realizations are needed to adequately sample the work distribution, given the experimental broadening of the force histograms with an average dissipated work of >50 kT. As such, it seems imperative to rely on linkers that are as short as possible to probe surface to molecule bonds. Based on our data both PEG_{600} and PEG_{2000} seem suitable.

Considering practical experimental aspects of SM-AFM, it seems hence necessary to aim for a compromise between tether length and convergence behavior. Too short tethers make it impossible to separate the primary minimum and the single molecule signature. Long linker will require a practically not feasible number of samples. Here, PEG_{600} is still experimentally feasible due to the small primary adhesive minimum. PEG_{2000}

DOI: 10.1021/acs.langmuir.7b02844
Langmuir 2018, 34, 766−772

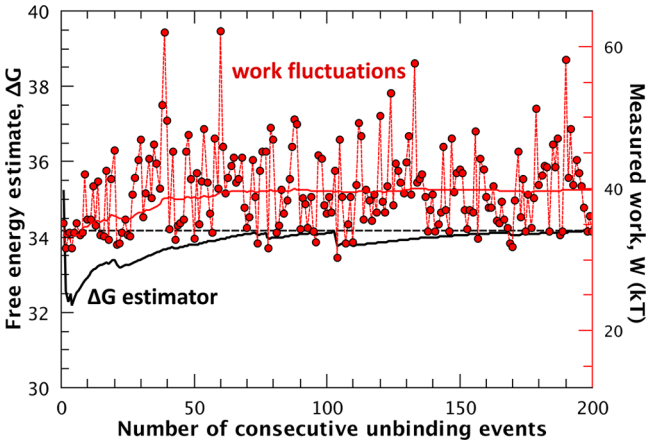

Figure 6. Comparison of work fluctuations and JE estimated free energies ΔG_0 as a function of recorded force trajectories for PEG_{600}. The solid red line indicates the evolution of the work average, and the dashed line indicates the converged free energy estimate (cf. text for details).

gives a bias 4−7 k_BT or 10−15%, and longer PEG molecules do not provide acceptable estimates for ΔG_0 within the given sampling of 200 trajectories. It also seems possible to further converge PEG_{2000} data. Anything up to $\sim 10^4$ realizations seems feasible in an experimental AFM setting.

CONCLUSIONS

In summary, our data provide an experimental characterization for biases resulting from the application of JE to unidirectional, nonequilibrium SM-AFM measurements of surface-to-molecule bonds with PEG tethers of varying length. We find that the systematic bias is due to extension of PEG further out thermodynamic equilibrium for longer linker molecules.

This work highlights important aspects about how SM-AFM experiments should be designed in order to deliver reasonable estimates for ΔG_0 for molecule−surface interactions based on JE with a feasible sample of force trajectories. Particularly, the influence of the linker's length may lead to strongly biased interaction energies. In practice, a compromise between polymer length and sample size is hence essential. Here, our data demonstrate that the shortest possible linkers are beneficial and converge within some 100 force trajectories. For the amine/gold bond there is a regime of linker lengths below 20 nm where the bias is <10−15% leading to reasonable estimates for ΔG_0. With longer linkers apparent methodical limits of the method are reached.

As a final aspect, our results also provide interesting insight into adhesion in general. In all experiments shown here we probe the same type of interaction with constant interaction energy and unbinding kinetics. An increasing amount of work is needed in average to break an adhesive junction based on the same functional adhesive bond if it is tethered to longer molecules, leading to an increasing dynamic strength of an adhesive bond. As such, how energy dissipates during adhesive failure offers a promising strategy for improving adhesive strength, i.e., the resistance to failure under applied force.

AUTHOR INFORMATION

Corresponding Author

*E-mail: markus@valtiner.de and valtiner@iap.tuwien.ac.at.

ORCID

Markus Valtiner: 0000-0001-5410-1067

Author Contributions

[‖]These authors contributed equally.

Notes

The authors declare no competing financial interest.

ACKNOWLEDGMENTS

T.U. and L.M.O. acknowledge funding through the International Max-Planck Research School IMPRS-SURMAT. M.V. and C.K. acknowledge funding through the European Research Council (ERC) through project CSI.interface (#677363). Financial support through the "Deutsche Forschungsgemeinschaft" is gratefully acknowledged. We thank P. Schiller for valuable discussions.

REFERENCES

(1) Florin, E. L.; Moy, V. T.; Gaub, H. E. Adhesion Forces between Individual Ligand-Receptor Pairs. *Science* **1994**, *264* (5157), 415−417.

(2) Moy, V. T.; Florin, E. L.; Gaub, H. E. Intermolecular Forces and Energies between Ligands and Receptors. *Science* **1994**, *266* (5183), 257−259.

(3) Lee, G. U.; Kidwell, D. A.; Colton, R. J. Sensing Discrete Streptavidin Biotin Interactions with Atomic-Force Microscopy. *Langmuir* **1994**, *10* (2), 354−357.

(4) Merkel, R.; Nassoy, P.; Leung, A.; Ritchie, K.; Evans, E. Energy Landscapes of Receptor-Ligand Bonds Explored with Dynamic Force Spectroscopy. *Nature* **1999**, *397* (6714), 50−53.

(5) Utzig, T.; Stock, P.; Valtiner, M. Resolving Non-Specific and Specific Adhesive Interactions of Catechols at Solid/Liquid Interfaces at the Molecular Scale. *Angew. Chem., Int. Ed.* **2016**, *55* (33), 9524−9528.

(6) Stock, P.; Monroe, J. J.; Utzig, T.; Smith, D. J.; Shell, M. S.; Valtiner, M. Unraveling Hydrophobic Interactions at the Molecular Scale Using Force Spectroscopy and Molecular Dynamics Simulations. *ACS Nano* **2017**, *11* (3), 2586−2597.

(7) Stock, P.; Utzig, T.; Valtiner, M. Soft Matter Interactions at the Molecular Scale: Interaction Forces and Energies between Single Hydrophobic Model Peptides. *Phys. Chem. Chem. Phys.* **2017**, *19* (6), 4216−4221.

(8) Rief, M.; Gautel, M.; Oesterhelt, F.; Fernandez, J. M.; Gaub, H. E. Reversible Unfolding of Individual Titin Immunoglobulin Domains by Afm. *Science* **1997**, *276* (5315), 1109−1112.

(9) Wang, Y.; Sischka, A.; Walhorn, V.; Tonsing, W.; Anselmetti, D. Nanomechanics of Fluorescent DNA Dyes on DNA Investigated by Magnetic Tweezers. *Biophys. J.* **2016**, *111* (8), 1604−1611.

(10) Horstmeier, S.; Walhorn, V.; Anselmetti, D. Dynamic Afm Force Spectroscopy of DNA Using Fm Mode with Constant Excitation. *EPL* **2017**, *117* (3), 38005.

(11) Jarzynski, C. Nonequilibrium Equality for Free Energy Differences. *Phys. Rev. Lett.* **1997**, *78* (14), 2690−2693.

(12) Jarzynski, C. Equilibrium Free-Energy Differences from Nonequilibrium Measurements: A Master-Equation Approach. *Phys. Rev. E: Stat. Phys., Plasmas, Fluids, Relat. Interdiscip. Top.* **1997**, *56* (5), 5018−5035.

(13) Jarzynski, C. Work Fluctuation Theorems and Single-Molecule Biophysics. *Prog. Theor. Phys. Suppl.* **2006**, *165* (165), 1−17.

(14) Liphardt, J.; Dumont, S.; Smith, S. B.; Tinoco, I.; Bustamante, C. Equilibrium Information from Nonequilibrium Measurements in an Experimental Test of Jarzynski's Equality. *Science* **2002**, *296* (5574), 1832−1835.

(15) Alemany, A.; Mossa, A.; Junier, I.; Ritort, F. Experimental Free-Energy Measurements of Kinetic Molecular States Using Fluctuation Theorems. *Nat. Phys.* **2012**, *8* (9), 688−694.

(16) Gupta, A. N.; Vincent, A.; Neupane, K.; Yu, H.; Wang, F.; Woodside, M. T. Experimental Validation of Free-Energy-Landscape

DOI: 10.1021/acs.langmuir.7b02844
Langmuir 2018, 34, 766−772

Reconstruction from Non-Equilibrium Single-Molecule Force Spectroscopy Measurements. *Nat. Phys.* **2011**, *7* (8), 631−634.
(17) Raman, S.; Utzig, T.; Baimpos, T.; Shrestha, B. R.; Valtiner, M. Deciphering the Scaling of Single-Molecule Interactions Using Jarzynski's Equality. *Nat. Commun.* **2014**, *5*, 5539.
(18) Jarzynski, C. Rare Events and the Convergence of Exponentially Averaged Work Values. *Phys. Rev. E* **2006**, *73* (4), 046105.
(19) Halpern, N. Y.; Jarzynski, C. Number of Trials Required to Estimate a Free-Energy Difference, Using Fluctuation Relations. *Phys. Rev. E: Stat. Phys., Plasmas, Fluids, Relat. Interdiscip. Top.* **2016**, *93* (5), 052144.
(20) Lu, N. D.; Kofke, D. A. Accuracy of Free-Energy Perturbation Calculations in Molecular Simulation. Ii. Heuristics. *J. Chem. Phys.* **2001**, *115* (15), 6866−6875.
(21) Lu, N. D.; Kofke, D. A. Accuracy of Free-Energy Perturbation Calculations in Molecular Simulation. I. Modeling. *J. Chem. Phys.* **2001**, *114* (17), 7303−7311.
(22) Wu, D.; Kofke, D. A. Phase-Space Overlap Measures. Ii. Design and Implementation of Staging Methods for Free-Energy Calculations. *J. Chem. Phys.* **2005**, *123* (8), 084109.
(23) Wu, D.; Kofke, D. A. Phase-Space Overlap Measures. I. Fail-Safe Bias Detection in Free Energies Calculated by Molecular Simulation. *J. Chem. Phys.* **2005**, *123* (5), 054103.
(24) Collin, D.; Ritort, F.; Jarzynski, C.; Smith, S. B.; Tinoco, I.; Bustamante, C. Verification of the Crooks Fluctuation Theorem and Recovery of Rna Folding Free Energies. *Nature* **2005**, *437* (7056), 231−234.
(25) Zuckerman, D. M.; Woolf, T. B. Theory of a Systematic Computational Error in Free Energy Differences. *Phys. Rev. Lett.* **2002**, *89* (18), 180602.
(26) Friddle, R. W. Comment on "Experimental Free Energy Surface Reconstruction from Single-Molecule Force Spectroscopy Using Jarzynski's Equality". *Phys. Rev. Lett.* **2008**, *100* (1), 019801.
(27) Chai, L.; Klein, J. Large Area, Molecularly Smooth (0.2 Nm Rms) Gold Films for Surface Forces and Other Studies. *Langmuir* **2007**, *23* (14), 7777−7783.
(28) Dammer, U.; Popescu, O.; Wagner, P.; Anselmetti, D.; Guntherodt, H. J.; Misevic, G. N. Binding Strength between Cell-Adhesion Proteoglycans Measured by Atomic-Force Microscopy. *Science* **1995**, *267* (5201), 1173−1175.
(29) Hinterdorfer, P.; Dufrene, Y. F. Detection and Localization of Single Molecular Recognition Events Using Atomic Force Microscopy. *Nat. Methods* **2006**, *3* (5), 347−355.
(30) Utzig, T.; Stock, P.; Valtiner, M. Resolving Non-Specific and Specific Adhesive Interactions of Catechols at Solid/Liquid Interfaces at the Molecular Scale. *Angew. Chem., Int. Ed.* **2016**, *55*, 9524−9528.
(31) Burnham, N. A.; Chen, X.; Hodges, C. S.; Matei, G. A.; Thoreson, E. J.; Roberts, C. J.; Davies, M. C.; Tendler, S. J. B. Comparison of Calibration Methods for Atomic-Force Microscopy Cantilevers. *Nanotechnology* **2003**, *14* (1), 1−6.
(32) Utzig, T.; Raman, S.; Valtiner, M. Scaling from Single Molecule to Macroscopic Adhesion at Polymer/Metal Interfaces. *Langmuir* **2015**, *31*, 2722.
(33) Donaldson, S. H.; Utzig, T.; Gebbie, M. A.; Raman, S.; Shrestha, B. R.; Israelachvili, J. N.; Valtiner, M. Electrochemical Control of Specific Adhesion between Amine-Functionalized Polymers and Noble Metal Electrode Interfaces. *Mater. Corros.* **2014**, *65* (4), 362−369.
(34) Aradhya, S. V.; Nielsen, A.; Hybertsen, M. S.; Venkataraman, L. Quantitative Bond Energetics in Atomic-Scale Junctions. *ACS Nano* **2014**, *8* (7), 7522−7530.
(35) Hybertsen, M. S.; Venkataraman, L.; Klare, J. E.; Whalley, A. C.; Steigerwald, M. L.; Nuckolls, C. Amine-Linked Single-Molecule Circuits: Systematic Trends across Molecular Families. *J. Phys.: Condens. Matter* **2008**, *20* (37), 374115.
(36) Venkataraman, L.; Klare, J. E.; Tam, I. W.; Nuckolls, C.; Hybertsen, M. S.; Steigerwald, M. L. Single-Molecule Circuits with Well-Defined Molecular Conductance. *Nano Lett.* **2006**, *6* (3), 458−462.
(37) Marko, J. F.; Siggia, E. D. Stretching DNA. *Macromolecules* **1995**, *28* (26), 8759−8770.
(38) Kienberger, F.; Pastushenko, V. P.; Kada, G.; Gruber, H. J.; Riener, C.; Schindler, H.; Hinterdorfer, P. Static and Dynamical Properties of Single Poly(Ethylene Glycol) Molecules Investigated by Force Spectroscopy. *Single Mol.* **2000**, *1* (2), 123−128.
(39) Hummer, G.; Szabo, A. Free Energy Reconstruction from Nonequilibrium Single-Molecule Pulling Experiments. *Proc. Natl. Acad. Sci. U. S. A.* **2001**, *98* (7), 3658−3661.
(40) Hummer, G.; Szabo, A. Free Energy Surfaces from Single-Molecule Force Spectroscopy. *Acc. Chem. Res.* **2005**, *38* (7), 504−513.
(41) Gore, J.; Ritort, F.; Bustamante, C. Bias and Error in Estimates of Equilibrium Free-Energy Differences from Nonequilibrium Measurements. *Proc. Natl. Acad. Sci. U. S. A.* **2003**, *100* (22), 12564−12569.

DOI: 10.1021/acs.langmuir.7b02844
Langmuir 2018, 34, 766−772